Antimicrobial Loading into and Release from Poly(ethylene glycol)/Poly(acrylic acid) Semi-interpenetrating Hydrogels

Yong Wu,[1] Jing Liang,[1] Ferenc Horkay,[2] Matthew Libera[1]

[1]Department of Chemical Engineering and Materials Science, Stevens Institute of Technology, Hoboken, New Jersey 07030
[2]Section on Tissue Biophysics and Biomimetics, Program on Pediatric Imaging and Tissue Sciences, Eunice Kennedy Shriver National Institute of Child Health and Human Development, National Institutes of Health, Bethesda, Maryland 20892
Correspondence to: M. Libera (E-mail: mlibera@stevens.edu)

Received 26 June 2015; accepted 14 September 2015; published online 00 Month 2015
DOI: 10.1002/polb.23924

ABSTRACT: Electrostatic interactions within a semi-interpenetrating network (semi-IPN) gel can control the post-synthesis loading, long-term retention, and subsequent release of small-molecule cationic antibiotics. Here, electrostatic charge is introduced into an otherwise neutral gel [poly(ethylene glycol) (PEG)] by physically entrapping high-molecular-weight poly(acrylic acid) (PAA). The network structure is characterized by small-angle neutron scattering. PEG/PAA semi-IPN gels absorb over 40 times more antibiotic than PAA-free PEG gels. Subsequent soaking in physiological buffer (pH 7.4; 0.15 M NaCl) releases the loaded antibiotics for periods as long as 30 days. The loaded gels elute antibiotics with diffusivities of 4.46×10^{-8} cm^2/s (amikacin) and 2.08×10^{-8} cm^2/s (colistin), which are two orders of magnitude less than those in pure PEG gels where diffusion is controlled purely by gel tortuosity. The release and hindered diffusion can be understood based on the partial shielding of the charged groups within the loaded gel, and they have a significant effect on the antimicrobial properties of these gels. © 2015 Wiley Periodicals, Inc. J. Polym. Sci., Part B: Polym. Phys. **2015**, *00*, 000–000

KEYWORDS: diffusion; hydrogels; poly(ethylene glycol); self-assembly; semi-interpenetrating network

INTRODUCTION Poly(ethylene glycol) (PEG)-based hydrogels have been widely studied for drug-delivery applications over several decades.[1] They have a 3D network structure that can control drug release while offering protection against the surrounding physiological environment.[2,3] Drug molecules incorporated during gel synthesis are eluted by tortuous diffusion through the gel matrix. This diffusion process can be controlled by the degree of gel swelling, crosslink density, and gel degradation rate.[4,5]

An alternate loading method relies on post-synthesis interactions between the hydrogel and the drug molecules. PEG-based gels, for example, can be created in the form of interpenetrating networks (IPNs)[5] or various copolymers,[6,7] and the inclusion of acrylic acid, acrylamide, or 2-hydroxyethyl methacrylate moieties[6] creates noncovalent interactions between the gel and drugs, which significantly affect drug uptake and release. Charged groups provide sites to which small molecules can bind. For example, electrostatic interactions of anionic molecules, for example, retinoic acid, indomethacin, and oligonucleotides, with the cationic network of crosslinked poly(ethylene oxide)/poly(ethylene imine) have been reported.[8] Similarly, we have previously demonstrated that introducing copolymerized acrylic acid into PEG microgels significantly enhances the loading of a cationic polypeptide into the microgel matrix.[3,9]

Here, we introduce electrostatic charge into a PEG gel by blending high-molecular-weight poly(acrylic acid) (PAA) with PEG diacrylate (PEGDA) to form a semi-IPN gel. Semi-IPN gels have been previously used to control drug release.[10–12] In contrast to this previous work, we investigate how electrostatic interactions can both enable post-synthesis antibiotic loading and control antibiotic release in different environments. We hypothesize that the PEG/PAA semi-IPN system will enhance cationic antimicrobial loading and that the subsequent release will depend on the prevailing electrostatic environment imposed by the surrounding medium. Two FDA-approved antibiotics, amikacin and colistin, with different size and cationic charge, are studied to explore the relationship between the gel network and the drug-release properties.

EXPERIMENTAL

Materials

Poly(ethylene glycol) diacrylate (PEGDA; $M_n = 575$ Da), PAA ($M_w = 450$ kDa), 2-hydroxy-2-methylpropiophenone (Darocur 1173), deuterium oxide, amikacin hydrate, colistin sulfate

salt, sodium chloride, sodium phosphate monobasic, sodium phosphate dibasic, potassium bromide, calcium chloride, magnesium chloride, Tryptic soy broth (TSB), Mueller Hinton Broth, and agar were purchased from Sigma Aldrich. All were used as received. Deuterated ethanol (ethanol-d_6; ETOD) was purchased from Cambridge Isotope Laboratories. Yeast extract and ethanol (99.5%, 200 proof) were purchased from Acros Organics. Dextrose (D-glucose) was purchased from Fisher Scientific. Type 1 water (18.2 MΩ) was used. *Staphylococcus aureus* [American Type Culture Collection (ATCC) 12600] was purchased from ATCC. *Escherichia coli* (NEB #C2987) was purchased from New England BioLabs.

Gel Preparation

PEG gels were synthesized by crosslinking 7 vol % PEGDA in water/ethanol (1:1; v:v) with photoinitiator (Darocur 1173; 0.02 vol %). After thorough mixing, 30 mL of this precursor solution was poured into a glass Petri dish and cured under a UV grid lamp for 15 min. Rectangular slabs (~1 cm × 1 cm × 0.5 cm) were cut from the resulting gel. To remove unreacted monomers and uncrosslinked oligomers, these slabs were soaked in deionized water for 1 week at which time UV absorption measurements indicated negligible elution from the gels. The gels were then dried overnight in air at 40 °C. Similarly, PEG/PAA gels were synthesized with 7 vol % PEGDA, 0.02 vol % photoinitiator, and 1 wt % PAA in water/ethanol (1:1; v:v).

Gel Swelling and Mesh Size

The pH response was determined by exposing dry gels to phosphate buffer (0.01 M) at pH values between 3 and 10 for 24 h. Response to varying salt concentrations was determined by exposing gels to phosphate buffer (0.01 M; pH 7.4) containing 0, 0.0015, 0.015, 0.15, and 1.5 M NaCl. Each experiment was performed three times. The gel swell ratio was defined as follows:

$$Q = \frac{1}{v_{2m}} = \frac{V_h}{V_d} \approx \frac{m_h}{m_d}, \quad (1)$$

where v_{2m}, V_h, V_d, m_h, and m_d are the volume fraction of polymer in the gel, the volume of the hydrated gel, the volume of the dry gel, the mass of the hydrated gel, and the mass of the dry gel, respectively. In a swollen network, the mesh size (ξ) is the average distance between adjacent crosslinks. For neutral gels, it can be calculated using the Flory-Rehner formulation:[13]

$$\xi = \left(\overline{r_0^2}\right)^{\frac{1}{2}} (v_{2m})^{-\frac{1}{3}}, \quad (2)$$

where $\left(\overline{r_0^2}\right)^{\frac{1}{2}}$ is the end-to-end distance of the network chains in the unperturbed state. $\left(\overline{r_0^2}\right)^{\frac{1}{2}}$ can be estimated from the characteristic ratio (C_n):

$$\left(\overline{r_0^2}\right)^{\frac{1}{2}} = C_n \frac{3M_c}{M_r} l^2, \quad (3)$$

where l is the weighted average bond length of C—C and C—O bonds (0.147 nm), C_n is 4.0 for PEG,[14] M_r is the molecular weight of the PEG repeating unit (44 g/mol), and M_c is the molecular weight between crosslinks. Based on the Flory-Rehner theory, M_c can be estimated from the following equation:

$$-[\ln(1-v_{2m}) + v_{2m} + \chi {v_{2m}}^2] = \left[\frac{v_l}{\bar{v} M_c}\right]\left[{v_{2m}}^{-\frac{1}{3}} - \frac{v_{2m}}{2}\right], \quad (4)$$

where $\bar{v}$ is the specific volume of PEG (0.893 cm^3/g), v_l is molar volume of water (18 cm^3/mol), and χ is the Flory-Huggins interaction parameter (0.426; ref. 15). Strictly speaking, eq 4 is not applicable for ternary polymer systems, such as the PEG/PAA gels, which contain two different polymers exhibiting both electrostatic and interpolymer interactions.

Small-Angle Neutron Scattering

Small-angle neutron scattering (SANS) measurements were made using the NG3 30 m instrument at the National Institute of Standards and Technology (NIST, Gaithersburg, MD). Gels were swollen in D_2O in 2-mm-thick sample cells. The cell consisted of 1-mm-thick quartz windows separated by a 2-mm spacer. The beam diameter was 20 mm. The measurements were made at sample-detector distances of 1.3, 4, and 13 m. This configuration covered the transfer wave-vector range of 0.002 $Å^{-1} < q < 0.3$ $Å^{-1}$, where $q = (4\pi/\lambda)\sin(\theta/2)$, and λ and θ are the wavelength of the incident radiation (0.8 nm) and the scattering angle, respectively. Counting times ranged from 20 min to 2 h. The total counts at the detector varied from 1 to 3 million. After radial averaging, corrections for detector response and for cell-window scattering were applied. The neutron-scattering intensities were calibrated using NIST absolute intensity standards.[16] The incoherent background was subtracted. All SANS experiments were carried out at 25 ± 0.1 °C.

Small-Molecule Loading

Dry PEG and PEG/PAA gels were exposed to amikacin or colistin loading solutions (1 mg/mL in 0.01 M phosphate buffer; pH 7.4). Samples of those solutions were then collected at 2-day intervals and transferred to a quartz 96-well microplate (Hellma). The amount of amikacin and colistin in these samples was determined by UV spectrophotometry with a microplate reader (BioTek) at 210 nm. The loading solutions were replaced with fresh solution once a decrease in the amount of antibiotic was detected. The total amount of amikacin or colistin loaded into the PEG or PEG/PAA gels after 9 days was calculated from the amount lost from the loading solution. Each experiment was performed three times for each group of samples.

Small-Molecule Release

Two eluting buffers (pH 7.4) were used: (1) low-salt buffer: 0.01 M phosphate; and (2) high-salt buffer: 0.01 M phosphate + 0.15 M NaCl. Fully hydrated antibiotic-loaded PEG and PEG/PAA gel slabs (1 cm × 1 cm × 2 mm) were exposed to these buffers (50 mL) for 30 days on an orbital shaker (60 rpm; USA Scientific). The medium was sampled every day for analysis. The eluting medium of 50 mL was replaced with fresh medium every 24 h. Amikacin and colistin release was assayed by UV spectrophotometry (210 nm). Each experiment was performed three times for each group. Control experiments used unloaded PEG and PEG/PAA hydrogels.

Antibiotic diffusion from the PEG/PAA semi-IPN gels into the high-salt buffer was modeled by Fick's Second Law. For the boundary conditions where the surface concentration is zero, the solute diffuses equally toward both faces of the gel slab, and diffusion from the slab edges is relatively small; the solution is given by:[17,18]

$$\frac{M_t}{M_\infty} = 1 - \sum_{n=0}^{\infty} \frac{8}{(2n+1)^2 \pi^2} e^{\frac{-(2n+1)^2 \pi^2 D t}{4L^2}}, \quad (5)$$

where M_t is the total cumulative mass released at time t, M_∞ is the total cumulative mass released at infinite time, M_t/M_∞ represents the fractional release,[18] L is the diffusion distance, and D is the solute (antibiotic) diffusivity. For long times, the solution can be approximated by:[19]

$$\frac{M_t}{M_\infty} = 1 - \frac{8}{\pi^2} e^{\frac{-\pi^2 D t}{4L^2}}. \quad (6)$$

Antibiotic diffusion through a chemically noninteractive gel depends on the swell ratio of the gel, Q, and the hydrodynamic radius of the solute, r_{drug}. The diffusivity was estimated by:[20]

$$\frac{D_{drug,gel}}{D_{drug,water}} = \left(1 - \frac{r_{drug}}{\xi}\right) e^{\frac{-Y}{Q-1}}, \quad (7)$$

where $D_{drug,gel}$ and $D_{drug,water}$ are the diffusivities in the swollen gel and in water and Y is a dimensionless constant ($\sim$1).[20,21] $D_{drug,water}$ was calculated using the Stokes-Einstein equation by:[22]

$$D_{drug,water} = \frac{k_B T}{6\pi\eta r_{drug}}, \quad (8)$$

where k_B is the Boltzmann constant, T is the temperature, and η is the viscosity of water.

Fourier Transform Infrared Spectroscopy

Hydrogel samples were freeze-dried, ground into powder, and then mixed with dehydrated potassium bromide (KBr) at a mass ratio of 1:20. Subsequently, the mixture was pressed into a pellet, and Fourier transform infrared (FTIR) spectra were acquired over wavenumbers of 750–3500 cm^{-1}.

In Vitro Antimicrobial Activity

The minimum concentration that inhibits 50% of the treated microorganisms (MIC_{50}) was determined using a protocol from the Clinical and Laboratory Standards Institute.[23] Cation-adjusted Muller Hinton broth supplemented with 25 mg/L of calcium and 12.5 mg/L of magnesium (CAMHB; 150 μL) with different amounts of amikacin and colistin was added to 96-well microplates by twofold serial dilution. Each well was inoculated with *S. aureus* or *E. coli* in CAMHB. The final antibiotic concentrations ranged from 0.008 to 512 μg/mL, and the test culture had a final concentration of 5×10^5 colony-forming units (CFU)/mL. The plates were incubated at 37 °C for 24 h, and the optical density of each well was measured at 600 nm. Each experiment was performed three times for each group.

Loaded hydrated gels (50 mg) were placed in the individual wells of 12-well plates. About 2 mL of *S. aureus* or *E. coli* bacterial suspension (5×10^5 CFU/mL) in TSB with 6 mg/mL yeast extract and 8 mg/mL glucose (TSB) was added. The plates were incubated for 24 h at 37 °C with gentle orbital shaking (60 rpm). The resulting bacterial suspensions were collected and analyzed by absorbance (600 nm). The optical densities were converted into CFU/mL, and the antimicrobial activities were determined relative to the growth on unloaded control samples.

Disc diffusion susceptibility tests of loaded gels were carried out by the agar-diffusion Kirby-Bauer method. Bacterial suspensions were inoculated at 10^8 CFU/mL on Mueller-Hinton's agar. Samples loaded with amikacin were tested with *S. aureus*, and samples loaded with colistin were tested with *E. coli*. After 24 h of incubation at 37 °C, the inhibition zone diameter was measured. Control experiments used unloaded PEG and PEG/PAA hydrogels.

Statistical Analysis

Statistical analysis was performed using one-way analysis of variables (ANOVA) followed by an *F*-test to evaluate differences between groups. $P < 0.05$ was considered statistically significant.

RESULTS

FTIR and Gel Swelling

Poly(ethylene glycol) hydrogels and PEG/PAA gels were synthesized by UV photopolymerization with or without, respectively, high-molecular-weight homopolymer PAA in the precursor mixture. FTIR spectroscopy was used to chemically characterize the compositions of the resulting gels [Fig. 1(A)]. Both gels display an intense peak at 1735 cm^{-1} corresponding to the carbonyl stretch from the ester groups of crosslinked PEGDA, as well as a peak at 1108 cm^{-1}, which corresponds to the C—O stretch within the PEG. Both gels also exhibit a peak at 1643 cm^{-1} from the alkenyl stretch of unreacted acrylate groups. These spectra indicate that the PEG gels lack the 1570 cm^{-1} peak characteristic of the PEG/PAA gels due to deprotonated carboxyl groups.

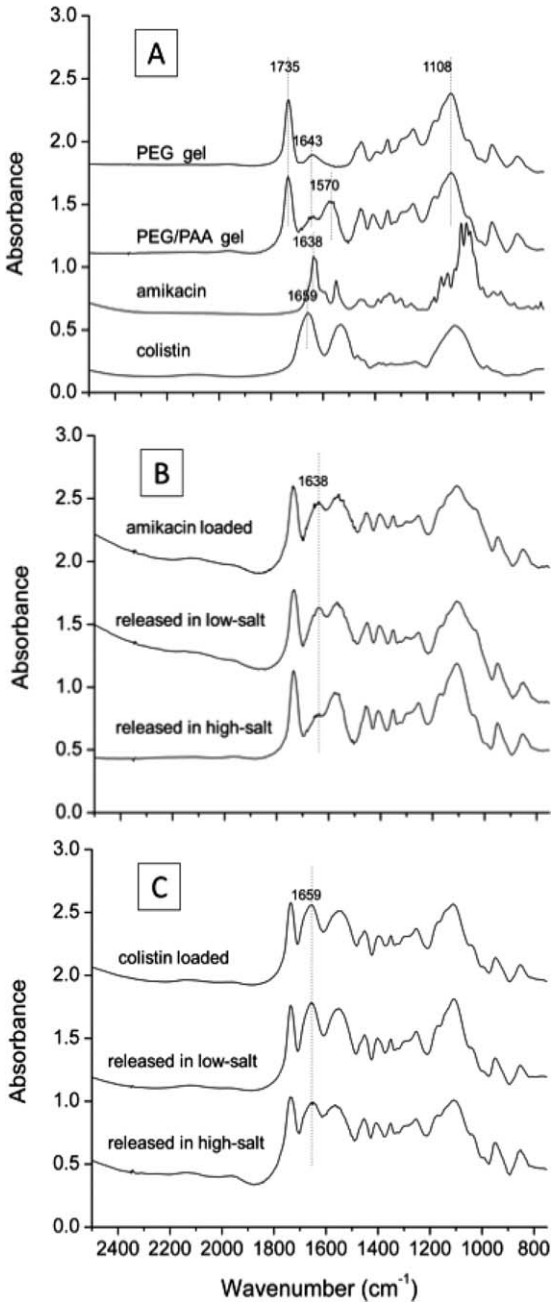

FIGURE 1 FTIR spectra of (A) pure components, (B) amikacin-loaded, and (C) colistin-loaded PEG/PAA semi-IPN gels as loaded and after 30-day immersion in low-salt phosphate buffer or high-salt buffer.

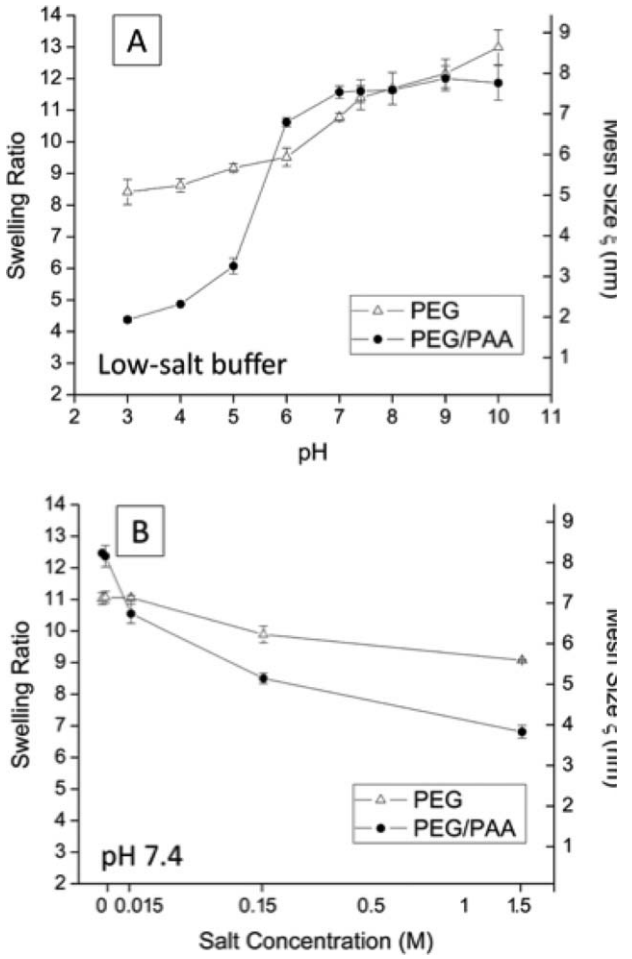

FIGURE 2 PEG and PEG/PAA gel swelling as a function of (A) pH and (B) NaCl concentration. Each datum corresponds to the mean, and the error bars correspond to the standard deviation of at least three measurements.

As the pendent PAA carboxyl groups are protonated below their pK_a of 4.5–5.0,[24–26] ionic repulsion increases the swell ratio of PEG/PAA gels as the pH is raised from 4 to 11 [Fig. 2(A)]. Similarly, at a constant pH of 7.4, introducing NaCl substantially reduces the PEG/PAA gel swelling relative to that measured in deionized water [Fig. 2(B)]. This effect results from the charge-screening effects of the additional cations.[27] It is less pronounced in the PEG gels [Fig. 2(B)], because the repulsive interactions between PEG moieties, primarily manifested through dipole interactions between ether oxygens, are much weaker than those between ionized acid groups. The formation of intermolecular complexes between PAA and poly(ethylene oxide)[28] below a pH of 3.8 may also contribute to the decreased swelling at low pH in the PEG/PAA gels.

The mesh size was estimated from the swelling data using eqs (1–4). For the PEG gel, this calculation yields $\xi \approx 6$–8 nm and increases slightly with increasing pH and decreasing salt concentration. The hydrodynamic diameter of PAA ($2R_g$) was estimated to be 40.5 nm.[29] As the calculated mesh size of the PEG gel is much smaller than the size of individual PAA molecules, we can expect that long-range movement of the high-molecular-weight PAA chains will be substantially hindered by the crosslinked PEG network.

Small-Angle Neutron Scattering

SANS was used to determine the effect of free PAA chains on the spatial organization of the PEG in the blended gels. Figure 3 shows SANS profiles for a PEG gel (+), a PEG/PAA gel

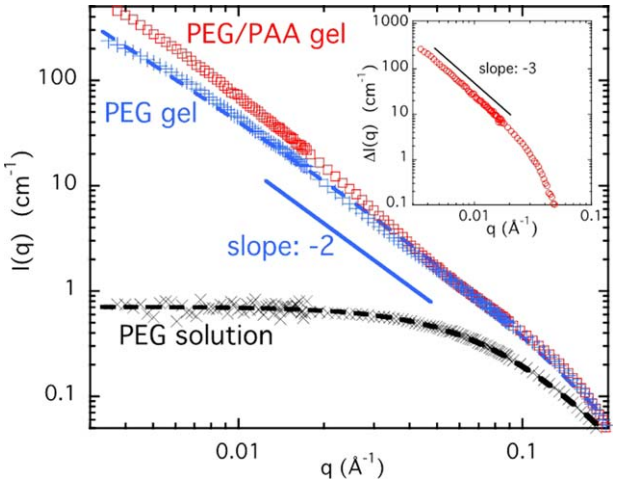

FIGURE 3 SANS profiles of PEG, PEG/PAA gels, and uncrosslinked PEG solution. The dashed curves are least squares fits of eq 9 to the data. The inset shows the difference signal $[\Delta I(q) = I(q)_{PEG/PAA} - I(q)_{PEG}]$ between PEG/PAA and PEG gels. [Color figure can be viewed in the online issue, which is available at wileyonlinelibrary.com.]

(□), and for a solution of the uncrosslinked PEG (×). The PEG content of the two gels and the solution was 5% (w/w). The PEG/PAA gel contained 1% PAA. The scattered intensity increases with increasing total polymer concentration and is greatest for the PEG/PAA gel. The gel curves exhibit similar features: at low q, the intensity decreases and displays a power-law scattering regime with a weak shoulder at higher values of q.

The high intensity for $q < 0.01$ Å^{-1} indicates cluster formation typical of gels. The cluster size exceeds 1000 Å and is beyond the SANS resolution. The slope in the low/intermediate q regions is about -2 and is due to scattering from clusters formed during photopolymerization. In the high q region ($q > 0.05$ Å^{-1}), the SANS intensity is governed by the polymer-chain geometry.

The scattering intensity from both gels is much stronger than that from the corresponding solution of the uncrosslinked linear PEG (575 Da). At low values of q, the intensity in the PEG solution is flat, and at $q \approx 0.08$ Å^{-1}, a shoulder is observed.

The greater intensity from the gels implies that crosslinking generates large structural nonuniformities that contribute to the scattering response at low q. At high q, the SANS profile is practically unaffected by the PAA chains. The inset (○) in Figure 3 shows the difference between the PEG/PAA and PEG gel signals $[\Delta I = I(q)_{PEG/PAA} - I(q)_{PEG}]$. The slope is about -3, corresponding to scattering from rough surfaces of large clusters.

The SANS spectra of the PEG gel were analyzed using the following equation, which reproduces the main characteristic features of the scattering curve:

TABLE 1 Parameters from SANS Profile Fits (eq 9) for a 5% PEG Gel and a 5% PEG Solution

Fitting parameter	PEG gel	PEG solution
ζ_i (Å)	75.7	15.5
A (cm^{-1})	0.71	3.2
B (cm^{-1})	0.014	–
n	1.8	–

$$I(q) = \frac{A}{[1+(q\zeta_i)^2]^{1/2}[1+q^2R_0^2]} + Bq^{-n}, \quad (9)$$

where ζ_i is the polymer–polymer correlation length, R_0 is the cross-sectional radius of the polymer, and A, B, and n are constants.[30] The intensity A is proportional to the average scattering contrast between the polymer and the solvent. The first term is governed by the thermodynamic concentration fluctuations, whereas the second term arises from large-scale static inhomogeneities frozen-in by the crosslinks. These large objects are not expected to make significant contribution to the thermodynamic properties of the system. Fits of eq 9 to the SANS data yield $\xi_{gel} = 7.5$ nm and $\xi_{sol} = 2.5$ nm, respectively (Table 1). The difference indicates the inhomogeneous distribution of the polymer in the crosslinked system. Note that ξ_{gel} is in excellent agreement with the value estimated from the swelling equilibrium data using the Flory-Rehner theory.

Antimicrobial Loading

Two FDA-approved antimicrobials, amikacin and colistin sulfate, were studied. Amikacin has an isoelectric point (pI) of 8.1 and a molecular weight of 586 g/mol. Colistin sulfate has a pI of 10.0 and a molecular weight of 1155 g/mol. In contrast to the high-molecular-weight PAA, the hydrodynamic diameters of amikacin ($2R_g \sim 1.14$ nm) and colistin ($2R_g \sim 1.44$ nm) are both much smaller than the gel mesh size, which enables penetration when the gels are immersed in an antibiotic solution.

The amount of antibiotic loaded into the gels was determined from the amount of antibiotic lost from the loading solution. This amount is given in Table 2 by the weight of loaded antibiotic relative to the weight of the dry gel before loading. PEG/PAA semi-IPN gels have substantially higher capacity than pure PEG gels. They can accommodate 42× more amikacin and 43× more colistin. The differences can be understood based on the electrostatic interactions in the two systems. At pH 7.4, the amikacin/colistin amine groups

TABLE 2 Amount of Loaded Antibiotic

Sample	Amount of amikacin (%, w/w)	Amount of colistin (%, w/w)
PEG gel	0.8 ± 0.1	1.3 ± 0.8
PEG/PAA gel	33.6 ± 0.2	56.6 ± 1.6

are both protonated, enabling strong electrostatic attraction of the cationic antimicrobials to the negatively charged PAA acid groups. The fact that slightly less amikacin loads than colistin can be attributed to colistin's higher isoelectric point and a higher total charge at pH 7.4.

FTIR spectroscopy confirms the antibiotic loading. In addition to spectra from pure PEG and PEG/PAA gels, Figure 1(A) shows the spectra from pure amikacin and pure colistin. These antimicrobials exhibit different C═O amide stretching, leading to distinct peaks at 1638 and 1659 cm^{-1} for amikacin and colistin, respectively. FTIR measurements confirm that little of either antibiotic load into the pure PEG gels. Spectra from amikacin-loaded and colistin-loaded PEG are indistinguishable from unloaded PEG gels (data not shown), as the small loading amounts (Table 2) challenge the sensitivity of FTIR spectroscopy. In contrast, the amikacin-loaded and colistin-loaded PEG/PAA gels clearly exhibit different absorbance spectra when compared with unloaded gels [Fig. 1(B,C)]. For amikacin-loaded gels, a peak at 1638 cm^{-1} corresponding to the amide stretching appears, but it overlaps with the PEG alkenyl C═C stretching at 1643 cm^{-1}. However, the incremental increase of intensity at this peak confirms the loading. Colistin-loaded gels display an additional peak at 1659 cm^{-1}.

Antimicrobial Release

Antibiotic release from PEG/PAA gels was studied using two different eluting buffers (pH 7.4): low-salt buffer (0.01 M phosphate) and high-salt buffer (0.01 M phosphate + 0.15 M NaCl). The buffers were refreshed daily, and thus, the gels were always in contact with solutions having a low antibiotic concentration.

Antimicrobial release was followed as a function of time by measuring the UV absorption of buffer solutions in which the loaded gels were immersed. The results are summarized in Figure 4. In low-salt buffer, except for an initial release of 10% amikacin and 2% colistin during the first 24 h, both antibiotics remain highly sequestered during 30 days of immersion. However, the addition of 0.15 M NaCl substantially changes the release profiles. About 98% of the loaded amikacin was released after 30-day immersion [Fig. 4(A)], and this can be attributed to Na^+ interference with the interaction between the $—COO^-$ groups of PAA and the $—NH_3^+$ groups of the amikacin.[31] Although this same shielding mechanism is active for the colistin-loaded PEG/PAA gels immersed in the high-salt buffer, the release rate and the total amount released after 30 days is less than that for amikacin. After a rapid release of 40% of colistin during the first 3 days, the colistin release follows a zero-order profile until Day 30 [Fig. 4(B)]. Over the entire period, roughly 92% of the loaded colistin is released. FTIR peaks at 1638 and 1659 cm^{-1} [Fig. 1(B,C)] confirm that amikacin and colistin are both retained in the PEG/PAA hydrogels after 30-day immersion in the low-salt buffer. For PEG/PAA gels soaked in high-salt buffer for 30 days, however, the amount of amikacin retained in the gels is below the FTIR detection limit. On the other hand, after 30-day immersion in high-salt buffer, the colistin-loaded PEG/PAA semi-IPN gels still exhibit a sharp band at 1659 cm^{-1} consistent with the UV measurements of cumulative release.

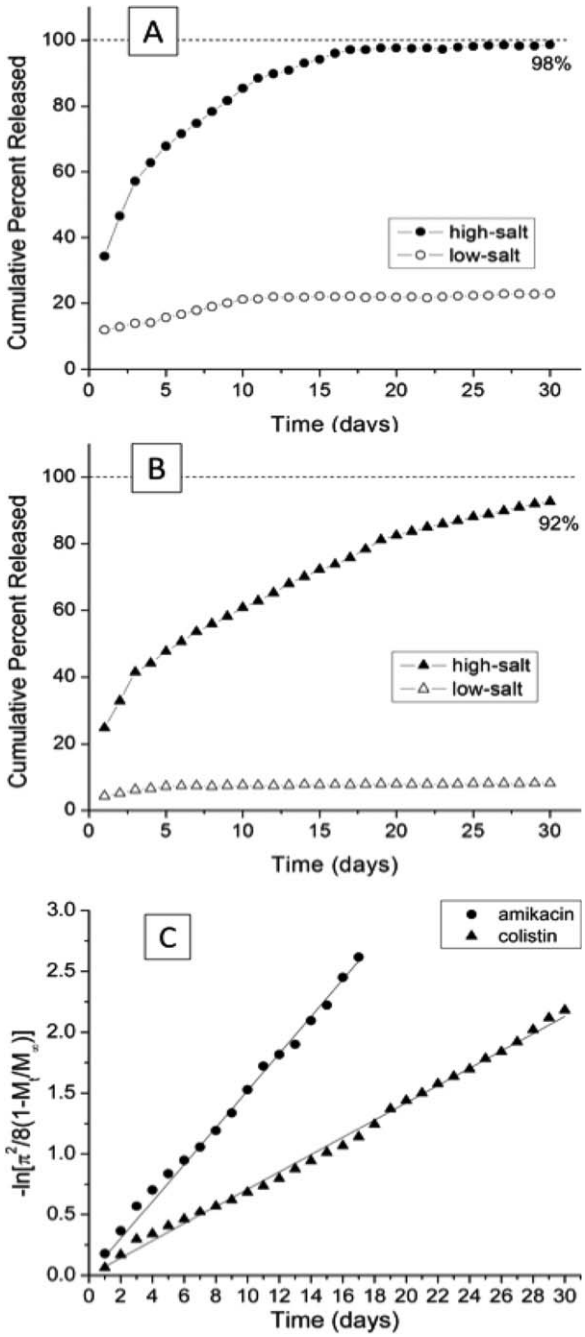

FIGURE 4 (A) Amikacin and (B) colistin release from PEG/PAA hydrogels in low- and high-salt buffer. (C) A Fickian model fits the antimicrobial release profiles with reduced diffusivities of amikacin and colistin elution into high-salt buffer.

The release profiles can be modeled [Fig. 4(C)] by the long-time solution of the diffusion equation (eq 6), with square correlation coefficients of 0.998 and 0.999 for amikacin and colistin, respectively. This model provides diffusivity values for amikacin and colistin in the PEG/PAA gels in high-salt buffer

of 4.46×10^{-8} and 2.08×10^{-8} cm^2/s, respectively. The differences can be attributed at least in part to differences in charge and size. Most importantly, colistin has a higher isoelectric point (pI $\sim$ 10), and more amine groups are protonated at pH 7.4 when compared with amikacin (pI $\sim$ 8.1). At pH 7.4, amikacin carries 3.3 positive charges, whereas colistin carries 5 positive charges. The average strength of the electrostatic interactions between colistin and the PAA are thus stronger than those between amikacin and PAA.

In Vitro Antimicrobial Activity

Amikacin, like most aminoglycosides, binds to the bacterial 30S ribosomal subunit, which causes misreading of mRNA and inhibits protein synthesis. Colistin sulfate is a polymyxin active against Gram-negative bacteria and has both hydrophilic and lipophilic moieties. Like a detergent, the hydrophobic/hydrophilic regions interact with the cytoplasmic membrane of Gram-negative bacteria, leading to membrane disruption. The MIC_{50} of amikacin was determined to be 0.5 μg/mL against *S. aureus*, and the MIC_{50} of colistin was determined to be 0.5 μg/mL against *E. coli*.

Figure 5 shows the results of *in vitro S. aureus* and *E. coli* culture in the presence of amikacin-loaded or colistin-loaded gels after they were immersed for 30 days in either low- or high-salt buffer. The gels were placed in TSB inoculated with either *S. aureus* or *E. coli* followed by overnight culturing. The OD of the medium above the antimicrobial-loaded PEG gels after culture was similar to the controls (unloaded gels soaked in low/high-salt buffer). As there is essentially no antimicrobial left in the PEG gels after 30-day immersion in buffer, these gels have little or no effect against either *S. aureus* or *E. coli*.

In contrast, PEG/PAA semi-IPN gels loaded with either amikacin or colistin are very effective against *S. aureus* or *E. coli* growth, respectively. Loaded PEG/PAA gels release only a fraction of their antibiotic payload when immersed in low-salt buffer (Fig. 5); however, the TSB medium provides salt that releases the cationic antimicrobials. These then elute from the gels and inhibit bacterial growth in the surrounding TSB. Similar effects are observed for loaded PEG/PAA gels after 30-day immersion in high-salt buffer (Fig. 5). Since during the immersion in high-salt buffer colistin release follows a zero-order profile, such release can continue when the gels are transferred to TSB. The colistin release rate into aqueous high-salt buffer is $\sim$0.38 mg/day [Fig. 4(B)] and yields a concentration in the TSB of 140 μg/mL, above the MIC_{50} of colistin to *E. coli*. Both the UV spectrophotometry measurements and FTIR spectra indicate that there is little amikacin retained in PEG/PAA gels after 30-day immersion in high-salt buffer. Nevertheless, *S. aureus* growth is inhibited when they are in proximity to these amikacin-loaded hydrogels [Fig. 5(A)]. By extrapolating the late-stage release profile in high-salt buffer [Fig. 4(A)], the amount of amikacin released in TSB is estimated as 14.9 μg/mL, which is again higher than the MIC_{50} of amikacin against *S. aureus*.

Amikacin-loaded or colistin-loaded PEG and PEG/PAA gels, after 30-day immersion in low-salt and high-salt buffers, were further tested for bacterial inhibition using the Kirby-Bauer assay (Fig. 6). None of the PEG gels exhibit an inhibition zone [Fig. 6(A,C)]. In contrast, both the amikacin-loaded and colistin-loaded PEG/PAA gels have inhibition zones with diameters that depend on both the type of antibiotic and the soaking conditions [Fig. 6(B,D)]. Consistent with the fact that most of the amikacin was previously released (Fig. 4), amikacin-loaded PEG/PAA gels produce a smaller inhibition zone (9.3 ± 0.1 mm diameter) against *S. aureus* than identical gels soaked in low-salt buffer (27.1 ± 0.1 mm diameter). Similarly, the colistin-loaded PEG/PAA gels soaked in low-salt buffer produce a zone diameter of 18.9 ± 0.4 mm against *E. coli*, whereas the ones in high-salt buffer produce a slightly smaller zone (14.9 ± 0.3 mm diameter).

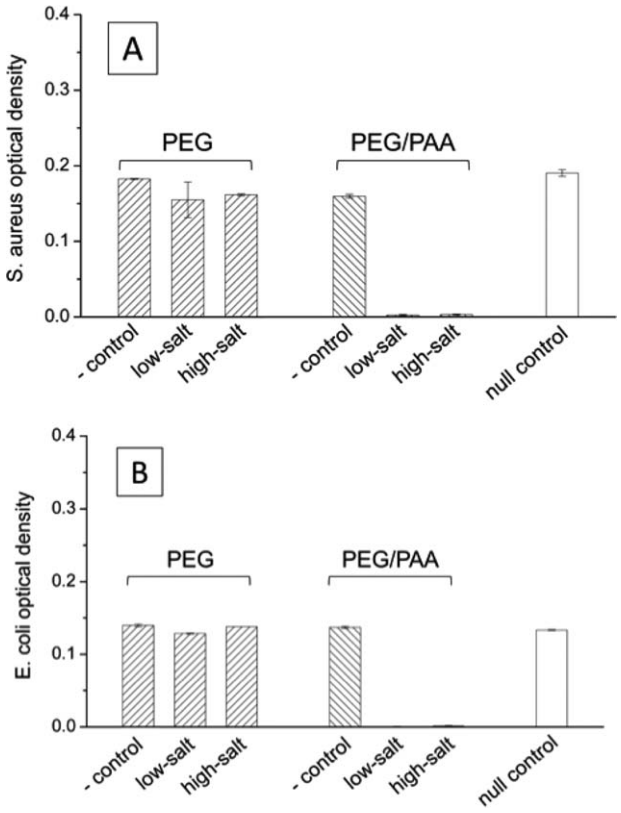

FIGURE 5 Optical density of (A) *S. aureus* suspension cultured with amikacin-loaded PEG and PEG/PAA hydrogels after 30-day release in low/high-salt buffer and of (B) *E. coli* suspension cultured with colistin-loaded PEG and PEG/PAA hydrogels after 30-day release in low/high-salt phosphate buffer. Control represents unloaded hydrogel; null control represents bacterial culture without any hydrogel.

DISCUSSION

Electrostatic interactions with the cationic antimicrobials are largely absent from the pure PEG gels. In these gels, the loading capacity is thus primarily controlled by concentration gradients that drive antibiotic diffusion into or out of the gel. The relatively small loading capacity of amikacin (0.8 wt %) and colistin (1.3 wt %) in the pure PEG gels (Table 2)

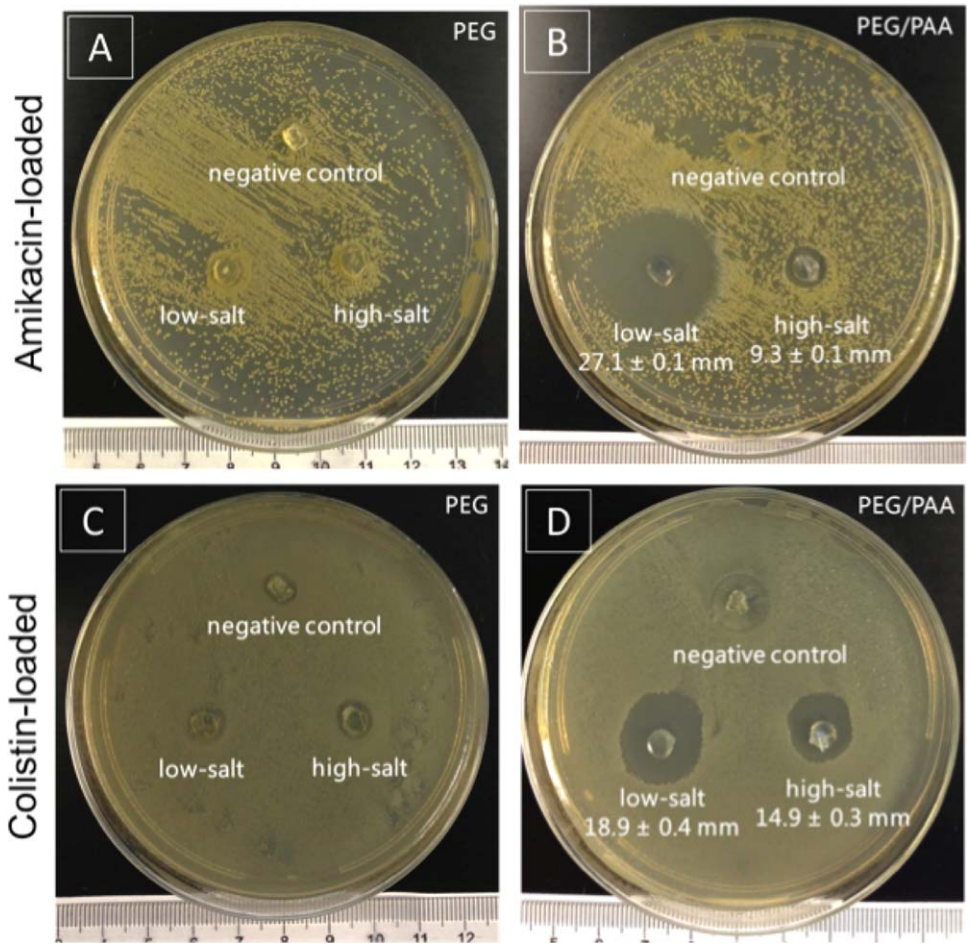

FIGURE 6 *S. aureus* inhibition zones by (A) amikacin-loaded PEG and (B) PEG/PAA gels, and *E. coli* inhibition zones by (C) colistin-loaded PEG and (D) PEG/PAA gels after 30-day immersion in low/high-salt buffer. Control corresponds to a soaked unloaded gel. [Color figure can be viewed in the online issue, which is available at wileyonlinelibrary.com.]

is about what can be expected when PEG gels are immersed in a 1 wt % solution. Antibiotic diffuses into the PEG gels until the concentrations inside and outside the gel are equal. The loading capacity is determined primarily by the antibiotic concentration of the loading solution subject to some additional but minor influence by dipole interactions between the cationic antimicrobials and the ether oxygens of the PEG. Unloading would proceed by the same mechanism, that is, diffusion down the concentration gradient from the loaded gel into the surrounding antibiotic-free solution.

The diffusivity associated with loading into and unloading from a noninteracting crosslinked network of a given mesh size can be estimated using eq 7. D_{water} can be approximated using the Stokes-Einstein equation to give 3.76×10^{-6} and 2.97×10^{-6} cm^2/s for amikacin and colistin, respectively. Taking into account the tortuosity associated with a PEG gel network, eq 7 yields noninteracting diffusivities D_{gel} of 1.2×10^{-6} and 0.95×10^{-6} cm^2/s, for amikacin and colistin, respectively. Tortuosity only reduces the diffusivities by a factor of about three. These values give a characteristic diffusion time ($L \sim \sqrt{Dt}$) into or out of a PEG gel slab with 2 mm thickness on the order of 10^3 s. In other words, whatever is loaded into pure PEG gels is largely released over times of a few hours of soaking in buffer and is relatively ineffective for the many-week local delivery of antibiotics.

In contrast, the antibiotic diffusivities measured in the PEG/PAA gels are two orders of magnitude lower than those characteristic of diffusion through the tortuous network of an otherwise noninteracting gel. Thus, despite the fact that a physiological salt concentration introduces electrostatic shielding that interferes with complexation between the cationic antibiotics and the polyanionic gels, sufficient interaction remains to substantially slow antibiotic transport within the gel. Unlike models addressing salt counterions interacting with weak polyelectrolytes,[32–34] both amikacin and colistin possess several primary amines, each of which can interact with multiple acid groups within a single PAA molecule or within several different PAA molecules. Consequently, to become completely free, multiple bonds must simultaneously be severed. Hence, the substantial drop in diffusivity can be understood as a modified random walk of antibiotic molecules within the PEG/PAA gels, that is, short periods of relatively free diffusion within the gel are separated by periods of little or no diffusion when an antibiotic is bound to one or more PAA molecules. A similar

mechanism has been proposed to explain the reduced diffusivity associated with drug transport through molecularly imprinted gels where intermittent binding to imprinted memory sites slows the average drug diffusivity.[35]

Electrostatically hindered diffusivities on the order of 3×10^{-8} cm^2/s give rise to substantially longer release times. A characteristic diffusion time $L \sim \sqrt{Dt}$ into or out of a PEG/PAA gel slab with 2 mm thickness is on the order of 10^6 s. This leads to effective antibacterial properties, which, as manifested by assays for both Gram-negative and Gram-positive bacteria, in these gels lasts upward of 4 weeks and will scale with the gel dimensions.

CONCLUSIONS

Electrostatic charge was introduced into a PEG hydrogel by polymerizing PEG diacrylate in the presence of high-molecular-weight PAA to form a semi-interpenetrating polymer network of PAA kinetically trapped in the gel network. The PEG/PAA swelling depends on both pH and salt concentration. The gels can be loaded by post-synthesis immersion in an antibiotic-containing buffer medium at pH 7.4. The PAA enables the gels to load ~40 times more antibiotic than comparable pure PEG gels, and the majority of this antibiotic remains loaded when the PEG/PAA semi-IPN gels are subsequently immersed in antibiotic-free buffer solution. Release is triggered by salt. However, a hundred-fold decrease in antibiotic diffusivity relative to that characteristic of tortuous diffusion through the mesh of pure PEG gels indicates that electrostatics play a controlling role in the PEG/PAA - antibiotic interactions despite the partial electrostatic shielding. This approach introduces a thermodynamic basis with which to control the diffusivity in addition to the traditional kinetic approaches based on gel tortuosity and raises interesting questions about the nature of the polyelectrolyte conformation within the gels and the role that small-molecule size, shape, and spatial distribution of charge has on interactions with that polyelectrolyte.

ACKNOWLEDGMENTS

This research project has been supported by the Army Research Office through grant no. W911NF-12-1-0331. F. Horkay acknowledges the support of the Intramural Research Program of the NICHD/NIH. The authors are grateful for access to neutron-scattering facilities at the National Institute of Standards and Technology (U.S. Department of Commerce) supported in part by the National Science Foundation under Agreement No. DMR-0944772. The authors thank Boualem Hammouda (NIST) and Yuan Gao (NIH/NIST) for their help with the SANS experiment.

REFERENCES AND NOTES

1 K. Knop, R. Hoogenboom, D. Fischer, U. S. Schubert, *Angew. Chem. Int. Ed. Engl.* **2010**, *49*, 6288–6308.

2 D. Steinhilber, S. Seiffert, J. A. Heyman, F. Paulus, D. A. Weitz, R. Haag, *Biomaterials* **2011**, *32*, 1311–1316.

3 Q. Wang, E. Uzunoglu, Y. Wu, M. Libera, *ACS Appl. Mater. Interfaces* **2012**, *4*, 2498–2506.

4 B. Amsden, *Macromolecules* **1998**, *31*, 8382–8395.

5 B. V. Slaughter, S. S. Khurshid, O. Z. Fisher, A. Khademhosseini, N. A. Peppas, *Adv. Mater.* **2009**, *21*, 3307–3329.

6 G. X. Tan, J. W. Liao, C. Y. Ning, L. Zhang, *J. Appl. Polym. Sci.* **2012**, *125*, 3509–3516.

7 O. Z. Fisher, N. A. Peppas, *Macromolecules* **2009**, *42*, 3391–3398.

8 S. V. Vinogradov, T. K. Bronich, A. V. Kabanov, *Adv. Drug Deliv. Rev.* **2002**, *54*, 135–147.

9 Y. Wu, Q. Wang, M. Libera, *Macromol. Symp.* **2013**, *329*, 35–40.

10 B. B. Mandal, S. Kapoor, S. C. Kundu, *Biomaterials* **2009**, *30*, 2826–2836.

11 X. M. Sun, J. Shi, Z. Z. Zhang, S. K. Cao, *J. Appl. Polym. Sci.* **2011**, *122*, 729–737.

12 Y. X. Zhang, F. P. Wu, M. Z. Li, E. J. Wang, *Polymer* **2005**, *46*, 7695–7700.

13 P. J. Flory, Principles of Polymer Chemistry; Cornell University Press: Ithaca, New York, **1953**.

14 F. W. Billmeyer, Jr., Textbook of Polymer Science; Wiley: New York, **1984**.

15 P. Kofinas, V. Athanassiou, E. Merrill, *Biomaterials* **1996**, *17*, 1547–1550.

16 S. R. Kline, *J. Appl. Crystallogr.* **2006**, *39*, 895–900.

17 N. A. Peppas, J. J. Sahlin, *Int. J. Pharm.* **1989**, *57*, 169–172.

18 M. Ali, S. Horikawa, S. Venkatesh, J. Saha, J. W. Hong, M. E. Byrne, *J. Controlled Release* **2007**, *124*, 154–162.

19 L. Serra, J. Domenech, N. A. Peppas, *Biomaterials* **2006**, *27*, 5440–5451.

20 S. R. Lustig, N. A. Peppas, *J. Appl. Polym. Sci.* **1988**, *36*, 735–747.

21 M. Biondi, S. Fusco, A. L. Lewis, P. A. Netti, *J. Mater. Sci.: Mater. Med.* **2013**, *24*, 2359–2370.

22 S. L. Hume, K. M. Jeerage, *J. Nanoparticle Res.* **2013**, *15*, 1–16.

23 National Committee for Clinical Laboratory Standards, Methods for dilution antimicrobial susceptibility tests for bacteria that grow aerobically. Approved Standard: M7-A5; NCCLS: Wayne, PA, **2000**.

24 M. Fujiwara, R. H. Grubbs, J. D. Baldeschwieler, *J. Colloid Interface Sci.* **1997**, *185*, 210–216.

25 A. Richter, G. Paschew, S. Klatt, J. Lienig, K. F. Arndt, H. J. P. Adler, *Sensors* **2008**, *8*, 561–581.

26 S. Jafari, H. Modarress, *Iran. Polym. J.* **2005**, *14*, 863–873.

27 Y. Zhao, J. Kang, T. W. Tan, *Polymer* **2006**, *47*, 7702–7710.

28 V. V. Khutoryanskiy, A. V. Dubolazov, Z. S. Nurkeeva, G. A. Mun, *Langmuir* **2004**, *20*, 3785–3790.

29 G. Miquelard-Garnier, C. Creton, D. Hourdet, *Soft Matter* **2008**, *4*, 1011–1023.

30 F. Horkay, P. J. Basser, A. M. Hecht, E. Geissler, *Macromolecules* **2012**, *45*, 2882–2890.

31 T. Hoare, R. Pelton, *Langmuir* **2008**, *24*, 1005–1012.

32 E. Y. Kramarenko, A. R. Khokhlov, K. Yoshikawa, *Macromolecules* **1997**, *30*, 3383–3388.

33 E. Y. Kramarenko, A. R. Khokhlov, K. Yoshikawa, *Macromol. Theory Simul.* **2000**, *9*, 249–256.

34 A. V. Dobrynin, M. Rubinstein, *Prog. Polym. Sci.* **2005**, *30*, 1049–1118.

35 S. Venkatesh, J. Saha, S. Pass, M. E. Byrne, *Eur. J. Pharm. Biopharm.* **2008**, *69*, 852–860.